RESULTS FROM THE CHORUS EXPERIMENT

Maria-Gabriella Catanesi
CERN
CH1211, Geneva, Switzerland

Representing the CHORUS Collaboration

ABSTRACT

Recent results from the CHORUS (**C**ern **H**ybrid **O**scillation **R**esearch apparat**US**) experiment are summarized. CHORUS is an experiment designed to study neutrino oscillations using the pure and intense Wide Band ν_μ beam at SPS (CERN). A fraction of the neutrino interactions collected during the years 1994–1996 by the CHORUS experiment has been analyzed, searching for ν_τ charged current interactions, followed by the τ lepton decaying into a negative hadron or into a muon. Within the applied cuts, no ν_τ candidate has been found. This result leads to a 90% C.L. limit $P(\nu_\mu \rightarrow \nu_\tau) < 6.0 \cdot 10^{-4}$ for the mixing probability. We also report on the first direct observation of a neutrino-induced charged current interaction with two subsequent decays of short-lived particles, which a complete analysis allows us to interpret as D_s^{+*} production, followed by the decay chain $D_s^{+*} \rightarrow D_s^+\gamma$, $D_s^+ \rightarrow \tau^+\nu_\tau$, and $\tau^+ \rightarrow \mu^+\nu_\mu\bar{\nu}_\tau$.

1 Introduction

The question of neutrino mass and stability remains one of the most interesting in the actual physics scenario. This question is particularly relevant for the ν_τ, a member of the third generation of fermions, and one of the most promising candidates for Dark Matter in the universe.

Stimulated by these considerations, a new generation of accelerator experiments was built in order to search, with improved sensitivities, for $\nu_\mu \rightarrow \nu_\tau$ oscillations.[1,2] The approach adopted by the CHORUS experiment was to use a visual technique that allows a direct observation of the τ decay topology. The experiment took data in the reoptimized and rebuilt CERN Wide Band ν_μ beam from April '94 to September '97 (see Ref. 3). The new beam presents a higher intensity ($> 2 \times 10^{13}$ protons/cycle) and a higher mean neutrino energy ($\langle E_{\nu_\mu} \rangle \approx 27$ GeV). The mean distance of the neutrino source from the detector is 600 m. This, together with the event statistics and backgrounds, fixes the sensitivity of the experiment. The aim is to explore mixing angles down to $\sin^2(2\theta) \sim 10^{-4}$ putting, in the case of the absence of a signal, a new limit of a factor of 20 better than the existing one (see Ref. 5).

2 The Detector

CHORUS is a "classic" appearance experiment. In fact, it was conceived to identify ν_τ by detecting the τ path and decay vertex. In particular, the aim is to isolate a "few" signal events coming from the charge current interactions

$$\nu_\tau N \rightarrow \tau^- X, \tag{1}$$

followed by one of the decay topologies:

$$\begin{aligned} \tau^- &\hookrightarrow \mu^- \nu\nu && 18\%, \\ &\hookrightarrow h^- \nu + n\pi^0 && 50\%, \\ &\hookrightarrow h^- h^- h^+ + n\pi^0 && 14\%, \end{aligned}$$

and to separate these events from the large background of charged and neutral current interactions:

$$\begin{aligned} \nu_\mu N &\rightarrow \mu^- X, \\ \nu_\mu N &\rightarrow \nu_\mu X. \end{aligned}$$

Because of the very short τ^- decay length ($c\tau = 90$ μm), we need a precise device such as a nuclear emulsion to provide the required high-spatial resolution at the micron range.

The CHORUS target was made with 800 kg emulsion gel, segmented into four stacks of one radiation length each. Each stack was subdivided into 36 sheets. This configuration allows us fast, automatic, and semiautomatic scanning techniques [5] (developed at Nagoya University) which permit us to speed up the search time. Further improvements can be obtained by reducing the scanning area. This goal is reached by introducing, between the emulsion stacks, a scintillating fiber tracking detector which predicts the track's position at the stack exit.[6]

The detection of long-lived particles is done in CHORUS by using two magnetic spectrometers and a calorimeter (see Fig. 1). The first spectrometer, placed downstream from the target, consists of an array of three diamond-shaped fiber planes in a magnetic field of 0.12 T generated by a hexagonal air-core magnet[7] operating in pulsed mode, that allows determination of the sign and momentum of low-energy particles (below 10 GeV).

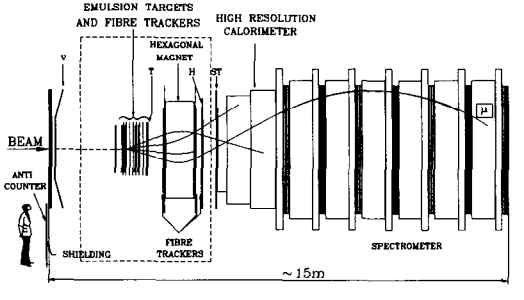

Figure 1: The CHORUS detector.

The second one, placed downstream from the calorimeter, is a "classic" muon spectrometer that allows measurement of the momentum of muons up to 100 GeV/c, with

a resolution of 20% at 75 GeV/c. It consists of six circularly magnetized iron modules with a magnetic field of 1.8 T, interleaved with a tracking section composed of drift chambers and streamer tube planes. The CHORUS sampling calorimeter is the first large-scale application of the so-called "spaghetti technique."[8] It consists of a lead and scintillating fiber matrix optimized for compensation, with an equal response to electromagnetic and hadronic showers. A full description of the CHORUS detector can be found in Ref. 9.

3 Data Selection and Analysis

3.1 Data Collection and Selection Criteria

In the 1994–1997 period, CHORUS collected 2,271,000 triggers corresponding to 5.06×10^{19} protons on target. Of these, 458,601 have a muon identified in the final state (the so-called 1μ events) and 116,049 do not (the so-called 0μ events), and a vertex position compatible with one of the four emulsion target stacks.

All tracks that are associated with the interaction vertex, with an angle of less than 0.4 rad from the beam axis, and (in view of the large emulsion background of muons originating from a nearby secondary target) more than 0.05 rad from the direction of this target, are extrapolated downstream and selected for further analysis. These tracks are searched for in the emulsion if their charge is negative and their momentum is within the range of $0 \leq p_h \leq 20$ GeV/c and $0 \leq p_\mu \leq 30$ GeV/c for hadrons and muons, respectively.

3.2 Vertex Location in Emulsion

The various steps for finding the plate containing the vertex by means of fully automated microscopes are identical to those described in Refs. 10 and 11. They are independently applied to all of the selected tracks in the event, namely the muon for the 1μ events, and all the negative tracks for the 0μ events. A track which has been found in the interface emulsion sheets is followed upstream in the target emulsion using track segments reconstructed in the most upstream 100 μm of each plate until the track disappears. This plate is referred to as the vertex plate. The mean efficiency of this scan-back procedure is found to be $\sim 32\%$ and $\sim 42\%$ for 0μ and 1μ events, respectively. The scanning results are summarized in Table 1.

Table 1: Current status of the CHORUS analysis.

	1994	1995	1996
Protons on target	$0.81 \cdot 10^{19}$	$1.20 \cdot 10^{19}$	$1.38 \cdot 10^{19}$
Emulsion triggers	422,000	547,000	617,000
1μ to be scanned	66,911	110,916	129,669
0μ to be scanned	17,731	27,841	32,548
1μ scanned so far	42,154	49,912	72,615
0μ scanned so far	8,908	12,635	-
1μ vertex located	18,286	20,642	30,128
0μ vertex located	3,401	3,805	0

3.3 Decay Search

Once the vertex plate is defined, automatic microscopic measurements are performed to select events potentially containing a decay topology (kink). As a result of the progress made in scanning procedures and improved performance in speed of the scanning devices, different algorithms have been applied. They are described in Refs. 10 and 11, and briefly recalled here.

In the first procedure, the event is selected either when the scan-back track has a significant impact parameter with respect to the other predicted tracks, or when the change in the scan-back track direction between the vertex plate and the exit from the emulsion corresponds to an apparent transverse momentum, p_T, which is larger than 250 MeV/c. For selected events, and for those with only one predicted track, digital images of the vertex plate are recorded and analyzed offline for the presence of a kink.

The second procedure is restricted to the search of *long* decay paths. In this case, the vertex plate is assumed to contain the decay vertex of a charged parent particle produced in a more upstream plate. With this procedure, only kink angles larger than 0.025 rad are detected.

For the events selected by either one of these procedures, a computer assisted eye-scan is performed to assess the presence of a secondary vertex and to accurately measure its topology. A τ^- decay candidate must satisfy the following criteria:

1. the secondary vertex appears as a kink without black prongs, nuclear recoils, blobs, or Auger electrons;
2. the transverse momentum of the decay muon (hadron), with respect to the parent direction, is larger than 250 MeV/c (to eliminate the decays of strange particles);
3. the kink in the 0μ channel occurs within three plates downstream from the neutrino interaction vertex plate. Because of the lower background, the kink search in the muonic decay channel was extended to five plates, with an efficiency gain of about 8%.

No τ^- decay candidate has been found which satisfies this selection criteria.

3.4 Background Estimates

In this section, we discuss the expected background from known sources for both hadronic and muonic τ decay channels.

The sources of background for the hadronic τ decay channel are:

- the production of negative charmed particles from the antineutrino components of the beam. These events constitute background if the primary μ^+ or e^+ remains unidentified. We expect ~ 0.02 events from these sources;
- the production of positive charmed mesons in charged current interactions, if the primary lepton is not identified and the charge of the charmed particle daughter is incorrectly measured. We expect ~ 0.03 events from this source in the present sample;
- the associated charm production both in charged current (when the primary muon is lost) and neutral current interactions, when one of the charmed particles is not detected. In the present sample, the estimated background from this process, taking into account the total charged current cross section[12] and the upper limit for associated charm production in charged current interactions, is < 0.01 events;
- the main potential background to the hadronic τ^- decays is due to the so-called hadronic "white kinks," defined as one-prong nuclear interactions with no heavily ionizing tracks (*black* and *grey* tracks in emulsion terminology), and no evidence for nuclear break up (evaporation tracks, recoils, blobs, or Auger electrons). Published data, which allows the determination of the white kink interaction cross section, is scarce.[13,14] The main source of data is from a dedicated experiment with 4 GeV pions at KEK.[13]

  Since the experimental information on the p_T dependence is statistically poor at large values, a Monte Carlo simulation based on a modified version of FLUKA[15,16] has been performed. The results of this simulation are in good agreement with the KEK p_T-dependence measurement. We estimate with the current statistics a background of 0.5 events within three plates downstream from the primary vertex plate.

The main source of potential background in the muonic τ channel is charm production. We expect less than 0.1 events in the current sample from the antineutrino components of the beam

$$\bar{\nu}_\mu(\bar{\nu}_e)M \rightarrow \mu^+(e^+)D^-X,$$

followed by

$$D^- \rightarrow \mu^- X^0,$$

in which the $\mu^+(e^+)$ escapes detection, or is not identified.

The prompt ν_τ contamination of the beam[17] is a background common to both the hadronic and muonic decay channels. For the present sample, the expected background is much less than 0.1 events.

4 Results

4.1 Oscillation Sensitivity

In the usual approximation of a two-flavor mixing scheme, the probability of ν_τ appearance in an initially pure ν_μ beam can be expressed as

$$P_{\mu\tau}(E) = \sin 2t \cdot \int \Psi(E,L) \cdot \cdot \sin^2\left(\frac{1.27 \cdot \Delta m^2_{\mu\tau}(\mathrm{eV}^2) \cdot L(\mathrm{km})}{E(\mathrm{GeV})}\right) \cdot dL,$$

where E is the incident neutrino energy, L is the neutrino flight length to the detector, $\theta_{\mu\tau}$ is the effective $\nu_\mu - \nu_\tau$ mixing angle, $\Delta m^2_{\mu\tau}$ is the difference of the squared masses

of the two assumed mass eigenstates, and $\Psi(E, L)$ is the fraction of ν_μ with energy E originating at a distance between L and $L + dL$ from the emulsion target.

The τ^- channels considered in the present $\nu_\mu \to \nu_\tau$ oscillation search are (1) $\tau \to \mu$, (2) $\tau \to h$, (3) $\tau \to e$, and (4) $\tau \to \bar{\mu}$ (where the μ is not identified).

The expected number $N_{\tau i}$ ($i = 1, 2, 3, 4$) of observed τ^- decays into a channel of branching ratio BR_i is then given by

$$N_{\tau i} = BR_i \cdot \int \Phi_{\nu_\mu} \cdot P_{\mu\tau} \cdot \sigma_\tau \cdot A_{\tau i} \cdot \epsilon_{\tau i} \cdot dE, \tag{2}$$

with

- $BR_{(1\ or\ 4)} = BR(\tau \to \nu_\tau \bar{\nu}_\mu \mu^-) = (17.35 \pm 0.10)\%$ (see Ref. 18).
- $BR_2 = BR(\tau \to \nu_\tau h^- n h^0) = (49.78 \pm 0.17)\%$ (see Ref. 18);
- $BR_3 = BR(\tau \to \nu_\tau \bar{\nu}_e e^-) = (17.83 \pm 0.08)\%$ (see Ref. 18);
- Φ_{ν_μ} the incident ν_μ flux spectrum;
- σ_τ the charged current ν_τ interaction cross section;
- $A_{\tau i}$ the acceptance and reconstruction efficiency for the considered channel (up to the vertex plate location); and
- $\epsilon_{\tau i}$ the corresponding efficiency of the decay search procedure.

With proper averaging (denoted by $\langle\rangle$), $N_{\tau i}$ can also be written as a function of n_i

$$N_{\tau i} = BR_i \cdot n_i \cdot \langle P_{\mu\tau} \rangle \cdot \frac{\langle \sigma_\tau \rangle}{\langle \sigma_\mu \rangle} \cdot \frac{\langle A_{\tau i} \rangle}{\langle A_\mu \rangle} \cdot \langle \epsilon_{\tau i} \rangle, \tag{3}$$

where

- $n_1 = N_\mu$ (the number of located charged current ν_μ interactions corresponding to the considered event sample) and $n_2 = n_3 = n_4 = (N_\mu)_{0-\mu}$ (the product of N_μ and the relative fraction of the 0-μ sample for which the analysis has been completed);
- $\langle \sigma_{\mu(\tau)} \rangle = \int \frac{d\sigma_{\mu(\tau)}}{dE} \cdot \Phi_{\nu_\mu} \cdot dE$. It takes into account quasi-elastic interactions, resonance production, and deep-inelastic interactions $[\sigma(\frac{\langle \sigma_\tau \rangle}{\langle \sigma_\mu \rangle})_{syst.} \sim 7\%]$;
- $\langle A_{\mu(\tau i)} \rangle = \int \frac{d\sigma_{\mu(\tau)}}{dE} \cdot A_{\mu(\tau i)} \cdot \Phi_{\nu_\mu} \cdot dE$ $[\sigma(\frac{\langle A_{\tau i} \rangle}{\langle A_\mu \rangle})_{syst.} \sim 7\%]$;
- $\langle \epsilon_{\tau i} \rangle$ is the average efficiency of the decay search procedure for the accepted events $[\sigma(\langle \epsilon_{\tau i} \rangle)_{syst.} \sim 10\%]$;

Table 2: Quantities used in the estimation of the sensitivity.

	1994	1995	1996
N_μ	18,286	20,642	30,128
r_σ	1.89	1.89	1.89
r_A	0.93	0.93	0.93
$\langle A_{\tau\mu} \rangle$	0.39	0.39	0.39
$\langle A_{\tau h} \rangle$	0.17	0.17	–
$\langle A_{\tau e} \rangle$	0.093	0.093	–
$\langle A_{\tau\bar{\mu}} \rangle$	0.026	0.026	–
$\langle \epsilon_{\tau\mu} \rangle$	0.53	0.35	0.37
$\langle \epsilon_{\tau h} \rangle$	0.24	0.25	–
$\langle \epsilon_{\tau e} \rangle$	0.12	0.13	–
$\langle \epsilon_{\tau\bar{\mu}} \rangle$	0.22	0.23	–
N_μ^{eq}	11,987	12,743	–

To allow an easy combination of the results from 1-μ and 0-μ event samples, it is useful to define the "equivalent number of muonic events" of the 0-μ sample by

$$N_\mu^{eq} = (N_\mu)_{0-\mu} \cdot \sum_{i=2}^{4} \frac{\langle A_{\tau i} \rangle}{\langle A_{\tau\mu} \rangle} \cdot \frac{\langle \epsilon_{\tau i} \rangle}{\langle \epsilon_{\tau\mu} \rangle} \cdot \frac{BR_i}{BR_\mu}. \tag{4}$$

The 90% C.L. upper limit on the oscillation probability then simplifies to

$$P_{\mu\tau} \leq \frac{2.38 \cdot r_\sigma \cdot r_A}{BR_\mu \cdot \langle \epsilon_{\tau\mu} \rangle \cdot [N_\mu + N_\mu^{eq}]}, \tag{5}$$

where $r_\sigma = \langle \sigma_\mu \rangle / \langle \sigma_\tau \rangle$ and $r_A = \langle A_\mu \rangle / \langle A_{\tau\mu} \rangle$.

In the above formula, the numerical factor of 2.38 takes into account the total systematic error (17%), following the description given in Ref. 19. The systematic error is mainly due to the reliability of the Monte Carlo simulation on scanning procedures.

The estimated values of the quantities appearing in this expression are given in Table 2. No statistical errors are quoted since they are much smaller than the systematic uncertainties.

Using the present sample, the following 90% C.L. limit is obtained

$$P_{\mu\tau} \leq 6.0 \cdot 10^{-4}. \tag{6}$$

In a two-flavor mixing scheme, the 90% C.L. excluded region in the ($\sin^2 2\theta_{\mu\tau}$, $\Delta m^2_{\mu\tau}$) parameter space is shown in Fig. 2. The maximum mixing between ν_μ and ν_τ is excluded at 90% C.L. for $\Delta\, m^2_{\mu\tau} > 0.9\ \mathrm{eV}^2$; and large Δm^2 values are excluded at 90% C.L. for $\sin^2 2\theta_{\mu\tau} > 1.2 \cdot 10^{-3}$.

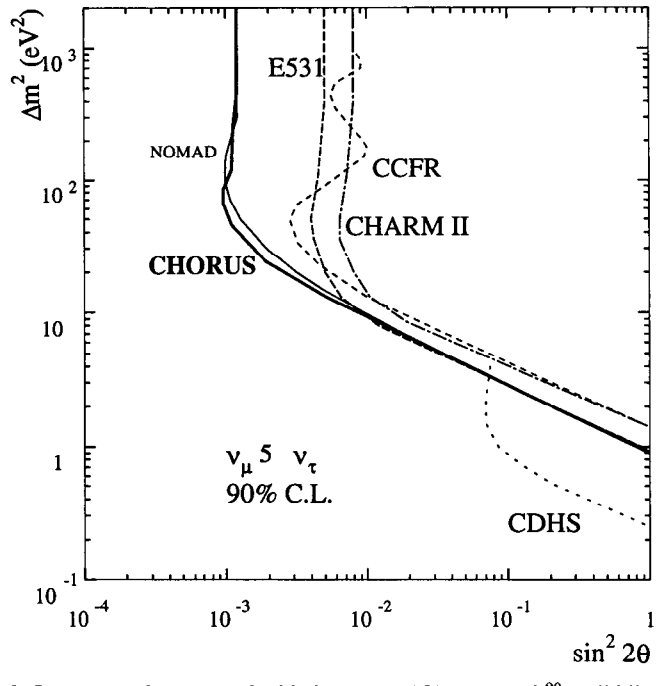

Figure 2: Present result compared with the recent NOMAD result[20] (solid line) and the previous limits (dotted lines).

4.2 The D_s^{+*} Observation

We have observed a neutrino-induced charged current interaction with two subsequent decays within 215 μm. A complete analysis of this event is possible because of the exceptional tracking capabilities of the CHORUS emulsion detector. Topological and kinematical reconstruction for the complete event are consistent with the decay chain

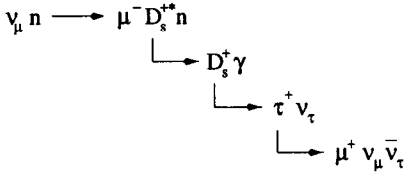

To find double kink events from the reaction $\nu_\mu N \to \mu^- D_s^+ (^* \to D_s^+ \gamma)(X^0)$, $D_s^+ \to \tau^+ \nu_\tau, \tau^+ \to \mu^+ \nu_\mu \bar{\nu}_\tau$, events with two opposite sign muons in the electronic detector are selected. To be sensitive to $D_s^{+*} \to D_s \gamma$ decays, we only allow electromagnetic energy in the calorimeter and veto hadronic activity. After finding the primary vertex, the event signature is manually examined for decay topologies with a double kink. One event recorded in the 1994 exposure fulfills all requirements for this event selection (see Fig. 3).

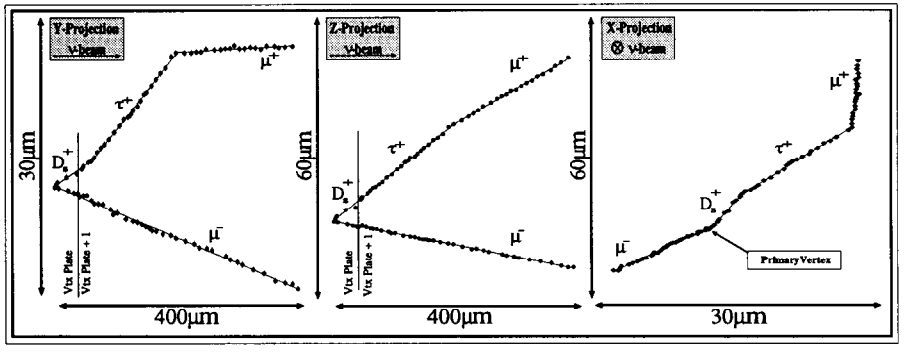

Figure 3: The double kink event in the emulsion.

In view of the short flight lengths with the measured momenta and decay angles, we assume the neutrino-induced production of a charmed particle (D or D_s meson) at the primary vertex. The probabilities for the different scenarios to take place and for detection in the CHORUS detector have been studied. The decay chain $D_s \to \tau \to \mu$ is clearly favored. Furthermore, the measured decay angles and momenta of the candidate event are consistent with this hypothesis.

Therefore, we may conclude that the observed double kink originates from the signature $D_s^+ \to \tau^+\nu_\tau$, $\tau^+ \to \mu^+\nu_\mu\bar{\nu}_\tau$.

At the primary vertex, no nuclear break up is observed. Low $Q^2 = (0.77 \pm 0.15)$ (GeV/c)^2 and the signal of a recoil neutron ($t = (0.89 \pm 0.39)$ (GeV/c)^2) point to a diffractive D_s^* production.

5 Conclusion

The emulsion scanning methods, previously described in Refs. 10 and 11, have been applied to a fraction of the 1994, 1995, and 1996 data. No τ^- decay candidate has been found, leading to a more stringent 90% C.L. upper limit on the $\nu_\mu \to \nu_\tau$ oscillation probability ($P_{\mu\tau} \leq 6.0 \cdot 10^{-4}$). During the second phase of the analysis (with better efficiencies, larger statistics, and faster automatic emulsion scanning), we plan to reach the design sensitivity ($P_{\mu\tau} \leq 1.0 \cdot 10^{-4}$).[1] The first direct observation of a neutrino-induced charged current interaction with a D_s^{+*} production detected at the vertex proves the exceptional capability of CHORUS in the detection of rare processes involving the decay of short-lived particles.

References

[1] CHORUS Collaboration, "A new search for $\nu_\mu \to \nu_\tau$," CERN/PPE/93-131.

[2] NOMAD Proposal, CERN-SPSC/91-21 (1991), SPSC P261 (1991).

[3] G. Aquistapace *et al.*, "The west area neutrino facility for CHORUS and NOMAD experiments: '94 to '97 operations," CERN/ECP/95-14.

[4] N. Ushida *et al.* (E531), Phys. Rev. Lett. **57**, 2897 (1986).

[5] S. Aoki *et al.*, "Fully automated emulsion analysis system, Nucl. Instrum. Methods B **51**, 466 (1990).

[6] S. Aoki *et al.*, "Scintillating fiber tracker with opto-electronics readout for the CHORUS neutrino experiment," Nucl. Instrum. Methods A **344**, 254 (1994).

[7] F. Bergsma *et al.*, "The hexagonal toroidal air-core magnet of the CHORUS detector," Nucl. Instrum. Methods A **357**, 243 (1995).

[8] S. Buontempo *et al.*, "Response to electrons and pions of the calorimeter for the CHORUS experiment," CERN-PPE/96-188, Nucl. Instrum. Methods A **378**, 222 (1996).

[9] E. Eskut *et al.*, CHORUS Collaboration, Nucl. Instr. Method A **401**, 7 (1997).

[10] E. Eskut *et al.*, CHORUS Collaboration, Phys. Lett. B **424**, 202 (1998).

[11] E. Eskut *et al.*, CHORUS Collaboration, Phys. Lett. B **434**, 205 (1998).

[12] N. Ushida *et al.*, E531 Collaboration, Phys. Lett. B **206**, 375 (1988).

[13] K. Kodama *et al.*, Fermilab P803 Proposal (1993), Appendix D.

[14] F. Baldassarre *et al.*, Nuovo Cimento XXI **3**, 459 (1961).

[15] A. Fassò, A. Ferrari, J. Ranft, and P. R. Sala, "New developments in FLUKA modelling of hadronic and EM interactions," in *Proceedings of the Third Workshop on Simulating Accelerator Radiation Environment,* SARE-3, KEK-Tsukuba, May 7–9, 1997, edited by H. Hirayama, KEK Report Proceedings 97-5, (1997) p. 32 .

[16] A. Ferrari, T. Rancati, and P. R. Sala, "FLUKA applications in high energy problems: from LHC to ICARUS and atmospheric showers," in *Proceedings of the Third Workshop on Simulating Accelerator Radiation Environment,*" SARE-3, KEK-Tsukuba, May 7–9 1997, edited by H. Hirayama, KEK Report Proceedings 97-5, (1997) p. 165 .

[17] B. Van de Vyver, Nucl. Instrum. Methods A **385**, 91 (1997).

[18] Particle Data Group, Phys. Rev. D **54**, 1 (1996).

[19] R. D. Cousins and V. L. Highland, Nucl. Instrum. Methods A **320**, 331 (1992).

[20] A. Marchionni for the NOMAD Collaboration, these Proceedings.